

Open Research Online

The Open University's repository of research publications and other research outputs

Theory of tunneling magnetoresistance in a disordered Fe/MgO/Fe(001) junction

Journal Item

How to cite:

Mathon, J. and Umerski, A. (2006). Theory of tunneling magnetoresistance in a disordered Fe/MgO/Fe(001) junction. *Physical Review B*, 74(14) p. 140404.

For guidance on citations see [FAQs](#).

© 2006 The American Physical Society

Version: Version of Record

Link(s) to article on publisher's website:
<http://dx.doi.org/10.1103/PhysRevB.74.140404>

Copyright and Moral Rights for the articles on this site are retained by the individual authors and/or other copyright owners. For more information on Open Research Online's data [policy](#) on reuse of materials please consult the policies page.

Theory of tunneling magnetoresistance in a disordered Fe/MgO/Fe(001) junction

J. Mathon¹ and A. Umerski²

¹*Department of Mathematics, City University, London EC1V 0HB, United Kingdom*

²*Department of Applied Mathematics, Open University, Milton Keynes MK7 6AA, United Kingdom*

(Received 5 July 2006; revised manuscript received 9 August 2006; published 20 October 2006)

Calculation of the tunneling magnetoresistance (TMR) of an Fe/MgO/Fe(001) junction with a disordered Fe/MgO interface is reported. It is shown that intermixing of Fe and Mg atoms at the interface decreases the TMR ratio rapidly and when about 16% of interfacial Fe atoms are substituted by Mg the calculated TMR saturates with increasing MgO thickness in good agreement with experiment. It is demonstrated that the saturation of TMR occurs because interfacial scattering leads to a redistribution of conductance channels, which opens up the perpendicular tunneling channel in the antiferromagnetic configuration that is forbidden for a perfect epitaxial junction.

DOI: [10.1103/PhysRevB.74.140404](https://doi.org/10.1103/PhysRevB.74.140404)

PACS number(s): 75.70.Cn, 75.45.+j

It was predicted theoretically^{1,2} that a very large tunneling magnetoresistance (TMR), in excess of 1000%, can be achieved for an epitaxial Fe/MgO/Fe(001) tunneling junction. Although recent measurements for this system³⁻⁵ give very large TMR ratios of the order of 300%, the situation remains somewhat controversial since there is one major aspect in which the theoretical results for a perfect Fe/MgO/Fe(001) junction differ fundamentally from the observed results. The theory predicts that the TMR ratio increases with increasing MgO thickness and there is no theoretical limit on the magnitude of TMR that can be achieved for a perfect epitaxial junction with a very thick MgO barrier. The calculated¹ dependence of the optimistic TMR ratio on MgO thickness is reproduced in Fig. 1(a) (broken curve). The TMR ratio increases with MgO thickness because symmetry impedes perpendicular tunneling of minority-spin electrons at the Γ point of the two-dimensional (2D) Brillouin zone.² When the tunneling conductance in the antiferromagnetic (AF) configuration is plotted in the 2D Brillouin zone it exhibits¹ a “hole” around the Γ point. This is illustrated in Fig. 1(b). It follows that the tunneling conductance in the AF configuration decays asymptotically exponentially with increasing MgO thickness at a rate higher than that in the ferromagnetic (FM) configuration in which tunneling of majority-spin electrons at the Γ point is allowed.

In contrast to these theoretical predictions, the experimental results of Yuasa *et al.*,³ which are also reproduced in Fig. 1 (circles), show a rapid saturation of TMR with increasing MgO thickness. It is essential to identify the physical mechanism that controls the observed saturation of TMR since we can then try to manipulate it to reach the desired theoretical regime in which TMR increases asymptotically monotonically with MgO thickness.

We propose that the physical mechanism that causes the saturation of TMR is a relatively small amount of disorder at one (or both) of the Fe/MgO interfaces. In particular, we shall show that intermixing of Fe and Mg atoms at one of the Fe/MgO interfaces can reproduce very well the observed behavior of TMR as a function of MgO thickness. Such intermixing of Fe and Mg atoms certainly takes place if a small amount of FeO is formed at the interface.⁶ The fact that the measured conductances³ are almost perfect straight lines when plotted against MgO thickness on a logarithmic scale

suggests that the MgO barrier itself is of a high quality. Even if there are imperfections in the bulk of MgO, it will be seen that they cannot explain the observed saturation of TMR. We shall therefore assume in our calculations that the MgO barrier is perfect.

The method of choice for investigating the effect of interfacial intermixing is a lateral supercell geometry. While the method is straightforward in principle, one encounters serious numerical problems when applying it to a disordered Fe/MgO/Fe(001) junction. The aim is to evaluate the conductances $\bar{\Gamma}^\sigma$ of electrons of spin σ tunneling through a disordered junction from the Kubo-Landauer formula¹ in a supercell geometry. As before,¹ we use tight-binding bands fitted to an *ab initio* band structure of Fe and the barrier is described by tight-binding bands fitted to the band structure of bulk MgO.⁷ For details of our tight-binding parametrization of the Fe/MgO/Fe(001) junction see Ref. 1. Previously,¹ we fixed the position of the common Fermi level E_F in the middle of the MgO gap of 7.6 eV. This is correct for a perfect epitaxial junction.^{8,9} However, when an interfacial intermixing is present metal-insulator gap states (MIGS) may form at the interface, and such states determine ultimately the position of E_F in the MgO gap.¹⁰ Without detailed knowledge of the nature of the MIGS, the position of E_F in the MgO gap cannot be determined from first principles. We therefore treat the position of E_F in the MgO gap as the only

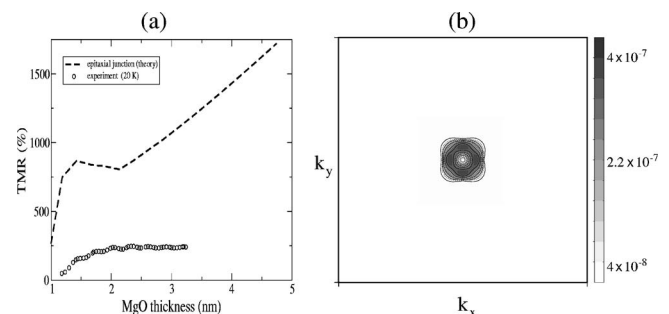


FIG. 1. (a) The computed TMR for a perfect epitaxial junction (broken curve) and the observed TMR (Ref. 3) (circles); (b) distribution in the two-dimensional Brillouin zone of the partial conductances in the antiferromagnetic configuration of the perfect epitaxial junction.

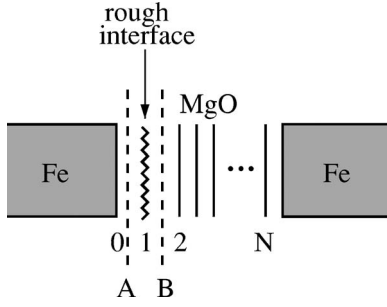


FIG. 2. Fe/MgO/Fe(001) junction with intermixing of Fe and Mg atoms at the left Fe/MgO interface; the two alternative positions of a cleavage plane are denoted by A and B.

parameter in our theory that is to be chosen so that the calculated absolute values of the tunneling conductances are the same as those measured by Yuasa *et al.*³ Once the position of E_F is fixed, the values of all the decay constants (effective heights of the gap) can be determined from the complex Fermi surface of MgO.¹

We use a mixed representation that is Bloch-like in the direction parallel to the layers and atomiclike in the perpendicular direction. We shall label all quantities in the supercell geometry with a tilde. The one-electron Green's functions \tilde{G} at the Fermi surface $E=E_F$, which are required in the Kubo formula, depend on the supercell wave vector \tilde{k}_{\parallel} parallel to the layers, plane index i , and indices r, s labeling atomic positions within the lateral cell. The Kubo formula in the lateral supercell geometry takes the form

$$\tilde{\Gamma}^{\sigma} = \frac{4e^2}{h} \sum_{\tilde{k}_{\parallel}, r} \text{Tr} \{ [\tilde{T}_{\sigma} \text{Im} \tilde{G}_L^{\sigma}(\tilde{k}_{\parallel}, r, r)] \cdot [\tilde{T}_{\sigma}^{\dagger} \text{Im} \tilde{G}_R^{\sigma}(\tilde{k}_{\parallel}, r, r)] \}. \quad (1)$$

The summation in Eq. (1) is over the supercell two-dimensional Brillouin zone and the cell index r . The trace is over the orbital indices corresponding to s, p, d orbitals that are required in a tight-binding parametrization of the junction. Finally, $\tilde{G}_L^{\sigma}(\tilde{k}_{\parallel}, r, s)$ and $\tilde{G}_R^{\sigma}(\tilde{k}_{\parallel}, r, s)$ are the one-electron Green's functions at the left (right) surfaces of a junction that is separated into two independent parts by an imaginary cleavage plane drawn between any two neighboring atomic planes L, R . Naturally, the total tunneling current in each spin channel is conserved and, therefore, it is immaterial in the calculation of TMR where the cleavage plane is positioned. However, it will be seen that for a physical interpretation of our results, it is convenient to place the cleavage plane in two alternative positions. These are denoted by A or B in Fig. 2, which shows schematically the junction we consider. We place the cleavage plane either immediately to the left of an interfacial atomic plane in which intermixing between Fe and Mg atoms is assumed to occur ($L=0, R=1$) or immediately to the right of this plane ($L=1, R=2$). The interface between MgO and the right Fe electrode is assumed to be perfect.

The separation of the junction into two independent parts is made simply for calculational purposes. The junction re-

mains physically connected and the interaction between the left and right parts is fully restored in Eq. (1) by the matrices \tilde{T}_{σ} and $\tilde{T}_{\sigma}^{\dagger}$ defined by

$$\tilde{T}_{\sigma} = \tilde{t}_{LR}(\tilde{k}_{\parallel}) [\tilde{I} - \tilde{G}_R^{\sigma}(\tilde{k}_{\parallel}) \tilde{t}_{LR}^{\dagger}(\tilde{k}_{\parallel}) \tilde{G}_L^{\sigma}(\tilde{k}_{\parallel}) \tilde{t}_{LR}(\tilde{k}_{\parallel})]^{-1}, \quad (2)$$

where \tilde{I} is a unit matrix and $\tilde{t}_{LR}(\tilde{k}_{\parallel})$ is the tight-binding hopping matrix connecting the surfaces L and R .

All the matrices in Eqs. (1) and (2) operate in a vector space that is a direct product of the space of atomic orbitals and the space of supercell indices r, s . For a typical 10×10 supercell, which we use here, the dimensions of all the matrices are 900×900 since nine orbitals are used in our tight-binding parametrization. We recall¹ that even calculations of the tunneling conductances for a perfect Fe/MgO/Fe(001) junction are numerically highly demanding since a very small imaginary part to the energy, of the order of 10^{-12} Ry, must be combined with a very fine mesh of \mathbf{k}_{\parallel} points to achieve convergence. We had to use in our original calculations¹ up to $\approx 10^6$ \mathbf{k}_{\parallel} points in the irreducible segment of the 2D Brillouin zone (BZ). When we tried to implement this program for a supercell with 900×900 matrices, the problem became numerically unstable. We have, therefore, developed an alternative strategy that not only delivers the required numerical accuracy but also gives a very clear physical interpretation of our supercell calculations.

To evaluate the Kubo formula, we first determined the surface Green's function $G_0^{\sigma}(\mathbf{k}_{\parallel})$ for the left Fe electrode (plane 0 in Fig. 2) and the surface Green's function $G_2^{\sigma}(\mathbf{k}_{\parallel})$ for the left surface of MgO deposited on the right Fe electrode (plane 2 in Fig. 2) using the simple cell basis. That involves only operations with matrices of the same small size as for a perfectly epitaxial junction. Only in the last step of "depositing" the mixed layer and connecting the left and right surfaces across the cleavage plane via Eq. (2) do we convert to the supercell basis. Such a conversion is possible since the simple and supercell bases span the same Hilbert space and there is, therefore, a unitary transformation $\tilde{M} = U M U^{-1}$ that transforms any matrix M with matrix elements $M(\mathbf{k}_{\parallel}, \mathbf{k}'_{\parallel})$ in the simple cell basis to a matrix \tilde{M} with matrix elements $\tilde{M}(\tilde{\mathbf{k}}_{\parallel}, \tilde{\mathbf{k}}'_{\parallel}, r, s)$ in the supercell basis, and vice versa (we suppress the orbital and plane indices since they remain the same in the simple and supercell representations). This method renders the calculation of the TMR for a disordered junction feasible.

To determine the TMR, we first calculated from Eqs. (1) and (2) the FM and AF tunneling conductances for different amounts of intermixing and performed a configuration average over 30 random configurations of Mg impurities. All the conductances we obtained are perfect straight lines when plotted on a logarithmic scale as a function of MgO thickness. Moreover, the tunneling conductance in the FM configuration $\tilde{\Gamma}_{FM}$ is quite insensitive to the amount of intermixing. The reason for this behavior will be explained later. We have, therefore, compared the slope of the calculated and observed³ conductances $\tilde{\Gamma}_{FM}$ to determine the position of E_F . The best fit is obtained for E_F lying about 2 eV above the top of the valence band of MgO. This value also represents the

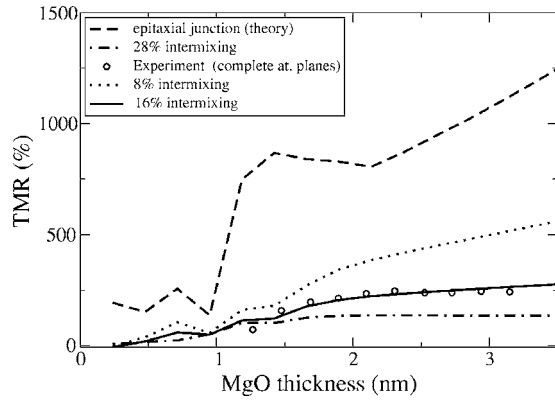


FIG. 3. The calculated TMR ratio for different amounts of intermixing between Fe and Mg atoms and the observed TMR ratio (circles).

effective height of a barrier for majority-spin electrons in the FM configuration. Using this value, we have calculated the TMR ratio for different amounts of intermixing between Fe and Mg atoms. The calculated results are compared in Fig. 3 with the experimental results of Yuasa *et al.*³ Since the TMR can only be calculated for thicknesses of MgO corresponding to complete atomic planes, we show in Fig. 3 the experimental results also for such discrete thicknesses (circles).

It can be seen that intermixing decreases the TMR ratio rapidly, and when some 16% of interfacial Fe atoms are substituted by Mg the calculated TMR saturates with MgO thickness in good agreement with the experiment.³

We now clarify the physical mechanism that causes the saturation. We propose that it is a redistribution of k_{\parallel} channels due to interfacial scattering that opens up the $k_{\parallel}=\mathbf{0}$ channel for one of the conductances in the AF configuration of the junction. It follows that the FM and AF conductances now decay exponentially with the MgO thickness at the same rate determined by the value of the imaginary wave vector in MgO at the Γ point. The saturation of TMR with MgO thickness is thus inevitable. To prove that this is indeed the correct physical mechanism of the saturation effect, we have applied the inverse of the unitary transformation $\tilde{M}=UMU^{-1}$ to the conductances $\tilde{\Gamma}^{\sigma}$, computed in the supercell geometry, to transform them back to the conductances Γ^{σ} which depend on k_{\parallel} from the ordinary BZ. This allows us to observe directly the aforementioned redistribution of k_{\parallel} channels and

examine in detail its effect on the conductances Γ^{σ} . Although $\Gamma^{\sigma}(k_{\parallel}, k'_{\parallel})$ is an off-diagonal matrix, only its diagonal elements determine the total conductance. This follows because the total conductance in the supercell representation given by Eq. (1) is a trace of the conductance matrix over all its indices (including \tilde{k}_{\parallel}) and the trace is invariant under the change of basis. It should be noted that the tunneling current in individual k_{\parallel} channels is no longer conserved across the rough interface and, therefore, the distributions of the partial conductances $\Gamma^{\sigma}(k_{\parallel}, k_{\parallel})$ in the 2D BZ are different for the two alternative positions A, B of the cleavage plane although the total conductance is conserved. Moreover, the partial conductances $\Gamma^{\sigma}(k_{\parallel}, k_{\parallel})$ are also conserved anywhere to the left (right) of the rough interface.

We first plot in Fig. 4 the dependence of all the conductances $\Gamma^{\sigma}(k_{\parallel}, k_{\parallel})$ on k_{\parallel} for the position B of the cleavage plane. The thickness of the MgO barrier is ten atomic planes and the concentration of Mg impurities in the rough interface is 16%. It can be seen that the conductances $\Gamma_{FM}^{\uparrow\uparrow}$, $\Gamma_{FM}^{\downarrow\downarrow}$, and $\Gamma_{AF}^{\uparrow\downarrow}$ are almost identical to those for a perfect junction shown in Fig. 3 of Ref. 1 (we use \uparrow, \downarrow to label the majority- and minority-spin carriers, respectively). However, $\Gamma_{AF}^{\downarrow\uparrow}$ shown in Fig. 4(d) is completely different since the “hole” at the Γ point, which exists for the perfect junction [see Fig. 1(b)], is removed for the disordered junction (note that $\Gamma_{AF}^{\downarrow\uparrow}=\Gamma_{AF}^{\uparrow\downarrow}$ for the perfect junction).

In Fig. 5 we show the conductances for the position A of the cleavage plane. The conductances $\Gamma_{FM}^{\uparrow\uparrow}$ and $\Gamma_{AF}^{\uparrow\downarrow}$ in Figs. 4 and 5 are almost identical. This is because \uparrow -spin carriers incident from the left Fe electrode can enter MgO at the Γ point regardless of whether the left interface is ordered or disordered, i.e., for majority-spin carriers disorder just leads to a redistribution of k_{\parallel} channels but does not affect the overall picture. However, the conductances $\Gamma_{FM}^{\downarrow\downarrow}$ and $\Gamma_{AF}^{\downarrow\uparrow}$ are very different for the two positions A and B of the cleavage plane. Figures 5(b) and 5(d) clearly demonstrate that \downarrow -spin carriers incident from the left Fe electrode with $k_{\parallel} \neq \mathbf{0}$ are scattered at the rough interface toward the Γ point where they can tunnel efficiently. In the case of $\Gamma_{FM}^{\downarrow\downarrow}$ the right interface prevents carriers with $k_{\parallel}=\mathbf{0}$ from propagating any further since there are no matching states for \downarrow -spin carriers in the right Fe electrode. Hence the hole at the Γ point in the conductance $\Gamma_{FM}^{\downarrow\downarrow}$ remains. On the other hand, in the case of $\Gamma_{AF}^{\downarrow\uparrow}$, \downarrow -spin carriers tunneling through MgO with the now allowed $k_{\parallel}=\mathbf{0}$ toward the right Fe electrode become \uparrow -spin carriers in that

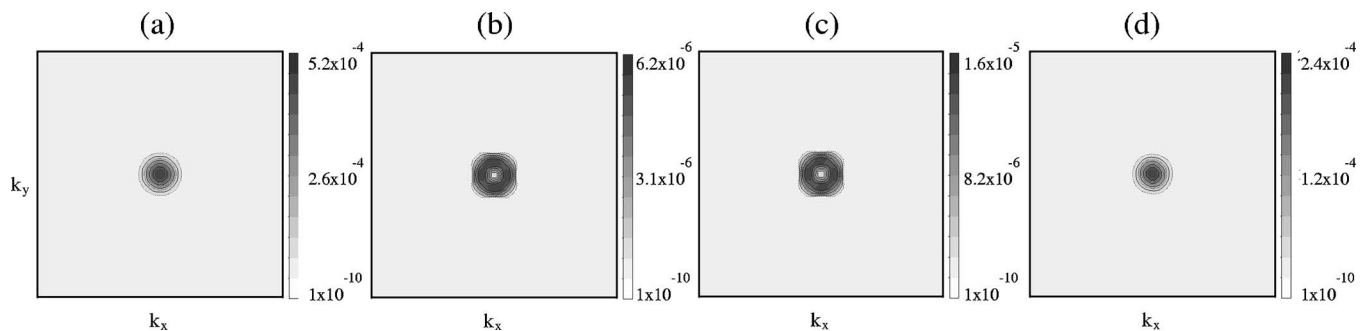


FIG. 4. Distribution of the partial conductances in the two-dimensional Brillouin zone for the position B of the cleavage plane: (a) $\Gamma_{FM}^{\uparrow\uparrow}$, (b) $\Gamma_{FM}^{\downarrow\downarrow}$, (c) $\Gamma_{AF}^{\uparrow\downarrow}$, (d) $\Gamma_{AF}^{\downarrow\uparrow}$.

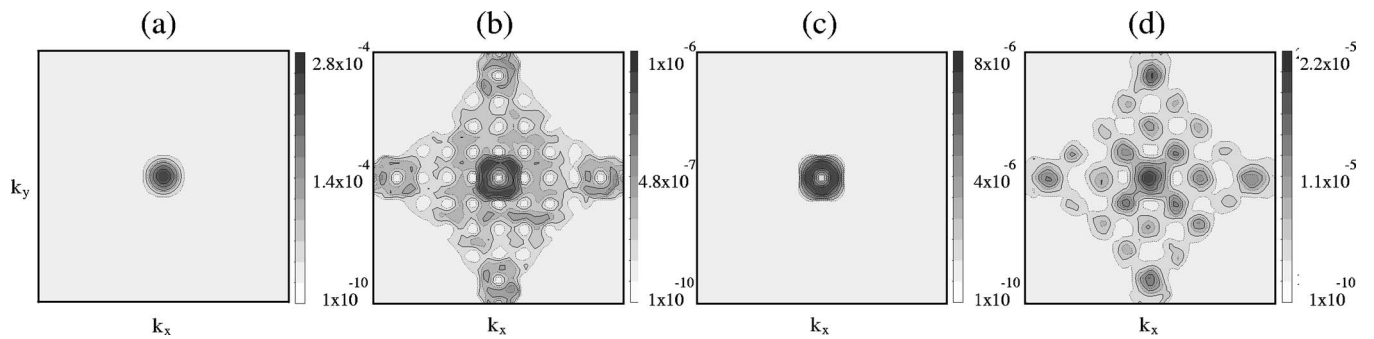


FIG. 5. Distribution of the partial conductances in the two-dimensional Brillouin zone for the position A of the cleavage plane: (a) $\Gamma_{FM}^{\uparrow\uparrow}$, (b) $\Gamma_{FM}^{\downarrow\downarrow}$, (c) $\Gamma_{AF}^{\uparrow\downarrow}$, (d) $\Gamma_{AF}^{\downarrow\uparrow}$.

electrode and can thus propagate at the Γ point across the whole junction. Therefore, the hole at the Γ point is removed. This demonstrates explicitly our argument that interfacial roughness removes the hole at the Γ point in the AF configuration. It should be noted that the “lattice” structure appearing in Figs. 5(b) and 5(d) is due to the finite size of our supercell. For a very large supercell, electrons from the whole cross section of the minority-spin surface spectral density of Fe(001) would contribute to tunneling.

It is appropriate to mention here that imperfections in the bulk of MgO cannot explain the saturation effect. This is because by the time \downarrow -spin carriers emitted from Fe at the Γ point reach an impurity in the bulk of MgO their wave functions have already decayed rapidly² and, hence, the Γ point \downarrow -spin conductance channel remains blocked. It is essential that scattering take place at (or very near) the interface so that \downarrow -spin carriers are scattered toward the Γ point just when they enter MgO [Fig. 5(d)] and can thus tunnel across the whole thickness of MgO with the same decay constant as \uparrow -spin carriers.

Finally, we shall briefly discuss the observed small oscillations of TMR with MgO thickness.³ Such oscillations could be fundamental since the complex Fermi surface of MgO has both imaginary and real sheets.^{2,3} The real part of the perpendicular wave vector in MgO could give rise to oscillations of TMR.^{2,11} However, since the MgO complex Fermi surface has no real part in a large region around the Γ point, this cannot be the correct explanation of the observed oscillations. Furthermore, the fact that the observed oscillations do not decrease with increasing MgO thickness is further evidence that they do not arise from the MgO complex

Fermi surface. On the other hand, it is clear that the amount of interfacial roughness varies periodically with MgO thickness and is smallest for thicknesses corresponding to most perfect interfaces. Since we have demonstrated that the magnitude of TMR depends critically on interfacial roughness, growth-induced oscillations of TMR with a period of approximately one atomic plane must occur. However, since the period of the observed oscillations is somewhat longer³ their precise origin requires further investigation.

We have demonstrated that a small amount of intermixing of Fe and Mg atoms at one of the Fe/MgO interfaces can explain the observed saturation of TMR with MgO thickness. It could be argued that one should also include in the rough interface an admixture of oxygen atoms to simulate small random regions of FeO. This would be desirable, and is possible in principle, but it would require very large lateral supercells, which would make reliable calculations of TMR much more difficult. However, it is clear from our discussion (see Figs. 4 and 5) that it is the existence of a disorder, rather than any particular type of disorder, that causes the saturation effect. It follows that other types of imperfection such as dislocations or oxygen vacancies would have qualitatively the same effect. Disorder at both interfaces gives qualitatively similar results but TMR saturates more rapidly.

Finally, the position of the Fermi level about 2 eV above the top of the valence band of MgO, which we deduced by comparing the calculated and measured³ tunneling conductances, is consistent with the height of the barrier quoted by Parkin *et al.*⁴ and with the weak bias dependence of TMR reported by Yuasa *et al.*³

¹J. Mathon and A. Umerski, Phys. Rev. B **63**, 220403(R) (2001).

²W. H. Butler, X. G. Zhang, T. C. Schulthess, and J. M. MacLaren, Phys. Rev. B **63**, 054416 (2001).

³S. Yuasa, T. Nagahama, A. Fukushima, Y. Suzuki, and K. Ando, Nat. Mater. **3**, 868 (2004).

⁴S. S. P. Parkin, Ch. Kaiser, A. Panchula, P. M. Rice, B. Hughes, M. Samant, and See-Hun Yang, Nat. Mater. **3**, 862 (2004).

⁵W. J. Gallagher and S. S. P. Parkin, IBM J. Res. Dev. **50**, No.1 (2006).

⁶C. Tusche, H. L. Meyerheim, N. Jedrecy, G. Renaud, A. Ernst, J. Henk, P. Bruno, and J. Kirschner, Phys. Rev. Lett. **95**, 176101

(2005).

⁷Ven-chung Lee and How-sen Wong, J. Phys. Soc. Jpn. **45**, 895 (1978).

⁸Chun Li and A. J. Freeman, Phys. Rev. B **43**, 780 (1991).

⁹W. Wulfhekel, M. Klauna, D. Ullmann, F. Zavaliche, J. Kirschner, R. Urban, T. Monchesky, and B. Heinrich, Appl. Phys. Lett. **78**, 509 (2001).

¹⁰M. W. Finnis, J. Phys.: Condens. Matter **8**, 5811 (1996).

¹¹J. Mathon, Murielle Villeret, and H. Itoh, Phys. Rev. B **52**, R6983 (1995).